

A TEM study and non-isothermal crystallization kinetic of tellurite glass-ceramics

El Sayed Yousef · A. E. Al-salami · E. R. Shaaban

Received: 22 February 2010/Accepted: 28 May 2010/Published online: 15 June 2010
© The Author(s) 2010. This article is published with open access at Springerlink.com

Abstract The glass transition temperature was studied via differential thermal analysis of glasses in the system $(100 - x)$ $\text{TeO}_2\text{--}5\text{Bi}_2\text{O}_3\text{--}x\text{ZnO}$ and $(100 - x)\text{TeO}_2\text{--}10\text{Bi}_2\text{O}_3\text{--}x\text{ZnO}$ where $x = 15, 20, 25$ in mol%. The crystallization behavior and microstructure development of the $0.7\text{TeO}_2\text{/}0.1\text{Bi}_2\text{O}_3\text{/}0.2\text{ZnO}$ glass during annealing were investigated by non-isothermal differential thermal analysis (DTA), X-ray diffractometry, and transmission electron microscopy. The glass transition temperature, crystallization temperature, and the nature of crystalline phases formed were determined. From the heating rate dependence of the glass transition temperature, the glass transition activation energy was derived. From variation of DTA peak maximum temperature with heating rate, the activation energies of crystallization were calculated to be 305.8 and 197 kJ mol^{-1} for first and second crystallization exotherms, respectively. Moreover, synthesized crystalline $\text{Bi}_{3.2}\text{Te}_{0.8}\text{O}_{6.4}$, $\text{Bi}_2\text{Te}_4\text{O}_{11}$, and $\text{Zn}_2\text{Te}_3\text{O}_8$ were investigated. In addition, the change in particle size with increasing annealing time was observed by high-polarized optical microscope.

Introduction

Nano-materials are considered as key technologies for this century. During the last 15 years, TeO_2 -based glasses have attracted much attention due to their linear and nonlinear refractive indices, excellent infrared transmittance. On the basis that, tellurium has an electronegativity in the range of other good glass forming oxide cations (Si, B, P, Ge, As, and Sb) [1–3]. Considerable interest has been generated by glass-ceramics that demonstrate optical second harmonic generation [4–6]. Kim et al. [7] proposed transparent TeO_2 -based glasses containing ferroelectrics crystals as a new type of nonlinear optical glass; he had been tried to fabrication transparent $\text{TeO}_2\text{--Li}_2\text{O}\text{--Nb}_2\text{O}_5$ glasses containing ferroelectrics LiNbO_3 crystals, always accompanied by another phase, which was considered to be a metastable pyrochlore-type compound. Kazuhide et al. [8] described a new cubic crystalline phase formed in $\text{TeO}_2\text{--K}_2\text{O}\text{--Nb}_2\text{O}_5$ glasses and glass-ceramic consisting of the phase that exhibits good optical at the wavelength of visible light. Komatsu et al. [9] obtained the crystalline phases in glass-ceramics of the $\text{TeO}_2\text{--Nb}_2\text{O}_5\text{--KTe}_2\text{O}$ depend on the valence of Te ions in the glassy state. The valence of Te^{4+} is easily oxidized to Te^{6+} ions and it retained for heat treatments at temperatures $\leq 600^\circ\text{C}$ [1]. Tromel et al. [10] obtained cubic face centered non-stoichiometric tellurites of lanthanides such as $\text{Ln}_2\text{Te}_6\text{O}_{15}$ and $\text{Ln}_4\text{Te}_7\text{O}_{15}$, in which Te ions are only Te^{4+} , by quenching homogeneous liquids at room temperature (i.e., the valence of Te in TeO_2 -based glasses is Te^{4+} affects the crystallization). Sato et al. [11] obtained the crystalline phases in glass-ceramics of the $\text{TeO}_2\text{--R}\text{O}\text{--Ln}_2\text{O}_3$ where R = Mg, Ba, Zn, and Ln = Sm, Eu, Er. Formed by laser irradiation are oriented at the surface. In our knowledge, few author have been fabricated TeO_2^{2-} based glasses to volume glass-ceramic because it is

E. S. Yousef (✉) · E. R. Shaaban
Physics Department, Faculty of Science, Al-Azhar University,
Assuit 71542, Egypt
e-mail: omn_yousef2000@yahoo.com

A. E. Al-salami
Physics Department, Faculty of Science, King Khalid University,
P.O. Box 9003, Abha, Saudi Arabia

Present Address:
E. S. Yousef
Physics Department, Faculty of Science, King Khalid University,
P.O. Box 9003, Abha, Saudi Arabia

difficult to get transparent TeO^{2-} based glass-ceramic. Recently, Senthil Murugan et al. [12] found that the study of vitreous phases obtained in the $(100 - 2x)\text{TeO}_2-x\text{Bi}_2\text{O}_3-x\text{ZnO}$, where $x = 5, 10$, and 15 system resulted in nonlinear optical application. They found these glasses exhibit SHG, which is about one-order of magnitude higher than that obtained for the fused silica glass. The objective of our article is to determine the preparation of transparent glasses and transparent glass-ceramics with a new composition $70\text{TeO}_2/10\text{Bi}_2\text{O}_3/20\text{ZnO}$, to characterize it by polarized optical microscope, TEM, DTA, and XRD, and finally to calculate the kinetic parameter, aiming to find the possible applications of this glass ceramics in optical devices.

Theoretical background

The theoretical basis for interpreting DTA results is provided by the formal theory of transformation kinetics as developed by Johnson and Mehl [13] and Avrami [14]. This theory describes the evolution with time, t , of the volume fraction crystallized, χ , in terms of the crystal growth rate u :

$$\chi = 1 - \exp \left[-gN_0 \left(\int_0^t u(t') dt' \right)^m \right], \quad (1)$$

where N_0 is the number of pre-existing nuclei per unit volume, n and m are kinetic exponents, which depends on the dimensionality of the crystal growth. In the considered case, “site saturation” [15], the kinetic exponent is $n = m$. Assuming an Arrhenian temperature dependence for $u = u_0 e^{E/RT'}$, and a heating rate, $\beta = \frac{dT}{dt}$, Eq. 1 becomes:

$$\begin{aligned} \chi &= 1 - \exp \left[-g \cdot N_0 \cdot u_0^n \cdot \beta^{-n} \left(\int_{T_0}^T e^{-E/RT'} dT' \right)^n \right] \\ &= 1 - \exp(-qI^n), \end{aligned} \quad (2)$$

where E is the effective activation energy for crystal growth. By using the substitution $y' = \frac{E}{RT'}$, the integral, I , can be represented, according to the literature [16], by the sum of the alternating series:

$$S'(y') = \left(\frac{-e^{-y'}}{y'^2} \right) \cdot \sum_{k=0}^{\infty} \frac{(-1)^k (k+1)}{y'^k}. \quad (3)$$

Considering that in this type of series the error produced is less than the first term neglected and bearing in mind that in most crystallization reactions $y' = \frac{E}{RT'} \gg 1$ [usually $\frac{E}{RT'} \geq 25$], it is possible to use the first term of this series, without making any appreciable error, and the above-mentioned integral becomes:

$$I = \left(\frac{E}{R} \right) \cdot e^{-y} \cdot y^{-2} = R \cdot T^2 \cdot E^{-1} \cdot \exp \left(\frac{-E}{RT} \right) \quad (4)$$

if $T_0 = T$ (where T_0 is the starting temperature) so that y_0 is infinite. This assumption is justifiable for any thermal treatment that begins at a temperature where crystal growth is negligible, i.e., below the glass transition temperature, T_g [17].

Substituting Eq. 3 into Eq. 2, the volume fraction crystallized in a non-isothermal process is expressed as:

$$\chi = 1 - \exp \left[-Q \cdot (K_R \cdot T^2 \cdot \beta^{-1})^n \right] \quad (5)$$

where $Q = g \cdot N_0 \cdot \left(\frac{R}{E} \right)^n$, a general expression for all values of the parameter n , which, as it is well known, in the case of “site saturation” depends on the mechanism of the crystal growth.

With the aim of calculating the kinetic parameters, the crystallization rate has been obtained by deriving Eq. 4 with respect to time, yielding:

$$\frac{dx}{dt} = n \cdot Q \cdot [k_R \cdot T^2 \cdot \beta^{-1}]^{n-1} \cdot (1 - x) \cdot [k_R \cdot E \cdot R^{-1} + 2k_R \cdot T], \quad (6)$$

which has been assumed that the reaction rate constant is a time function through its Arrhenian temperature dependence. The maximum crystallization rate is found by making $\frac{dx}{dt^2} = 0$, thus the relationship:

$$\left[\left(\frac{K_R \cdot \beta}{T_P^2} \right) \right]^n = 1 - \left(\frac{2}{n} \right) \cdot \left(1 + \frac{E}{RT_P} \right) \cdot \left(2 + \frac{E}{RT_P} \right)^{-2} \quad (7)$$

where the subscript, P , denotes the magnitude values corresponding to the maximum crystallization rate. Assuming the above-mentioned hypothesis $\frac{E}{RT_P} \gg 1$; the logarithmic form of Eq. 7 is written as:

$$\ln \left(\frac{T_P^2}{\beta} \right) = \frac{E}{RT_P} - \ln q = 0 \quad (8)$$

which is the equation of a straight line, whose slope and intercept give the activation energy, E , and the pre-exponential factor, $q = Q^{\frac{1}{n}} \cdot K_R$, respectively.

On the other hand, the quoted assumption, $\frac{E}{RT_P} \gg 1$, according to Eq. 4–6, allows us to express the maximum crystallization rate by the relationship:

$$\frac{dx}{dt}|_P = 0.37 \beta \cdot E \cdot n \cdot (RT_P^2)^{-1} \quad (9)$$

which makes it possible to obtain for each heating rate a value of the kinetic exponent, n . The corresponding mean value may be taken as the most probable value of the quoted exponent.

Experimental work

Glasses in the system $(100 - x)\text{TeO}_2 - 5\text{Bi}_2\text{O}_3 - x\text{ZnO}$ and $(100 - x)\text{TeO}_2 - 10\text{Bi}_2\text{O}_3 - x\text{ZnO}$ where $x = 15, 20, 25$ in mol% were prepared by mixing specified weights of raw material. Mixed batches were melted in gold crucible at 850 °C for ~30 min. The melt, which had a high viscosity, was cast at 700 °C in a graphite mold. Subsequently, the sample was transferred to an annealing furnace and kept for 2 h at 300 °C. Then, the furnace was switched off and the glass sample was allowed to cool. Samples for measurements of optical properties using DTA (Shimadzu DTA 50) curve of powdered specimen of about 30 mg were recorded in air at heating rate 3, 5, and 10 K min⁻¹, respectively, in Pt-crucible and using the same amount of Al_2O_3 as reference material in the range between 20 and 650 °C. The glass transition temperatures (T_g) is selected as mid-point between the onset and the minimum temperature, where T_c is measured at the onset of crystallization, the T_p is measured at the peak of crystallization.

X-ray diffraction (XRD) investigation were carried out in Siemens D 5000 using (CuK_α radiation) diffractometer at 40 kV and 40 mV setting in 2θ range from 10° to 90°. The crystallized phases were identified by comparing the peak position and intensities with those in the JCPDS (Joint Committee on Powder Diffraction Standards) date files. The volume crystallized sample was studied by TEM (Hitachi H8100) using 200 kV and optical sample was coated with carbon for TEM study. Optical microscopy (OM) investigation were performed in Zeiss Optimas equipped with Nikon Coolpix 4.0 MP digital camera.

Results and discussion

Homogeneous and transparent glasses were prepared in the system $(100 - x)\text{TeO}_2 - 5\text{Bi}_2\text{O}_3 - x\text{ZnO}$ and $(100 - x)\text{TeO}_2 - 10\text{Bi}_2\text{O}_3 - x\text{ZnO}$, where $x = 15, 20, 25$ in mol%. Differential thermal analysis (DTA) investigation was conducted on the as-cast prepared glasses. Figure 1 shows that, the glass transition temperature increase with increasing ZnO content, and also it increases with increasing Bi_2O_3 content in the glass matrix. T_g as a function of composition can reveal a transformation of the glass structure. We expect that, ZnO and Bi_2O_3 break down the TeO_4 network structure creating TeO_{3+1} and TeO_3 phase built in the glass matrix that results in the structural rearrangements of the glasses due to the transfer of the bridging oxygen into elongate bridging oxygen and non-bridging oxygen. The values of bond Te–O have four different kinds; Te–NBO_{ax}, Te–NBO_{eq}, Te–BO_{ax}, and Te–BO_{eq}, which is due to NBO with axial position, NBO with equatorial position, BO with axial position, and BO

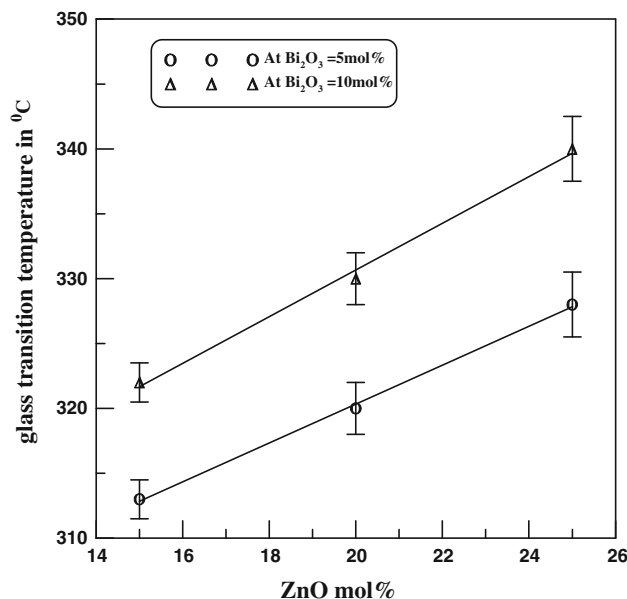
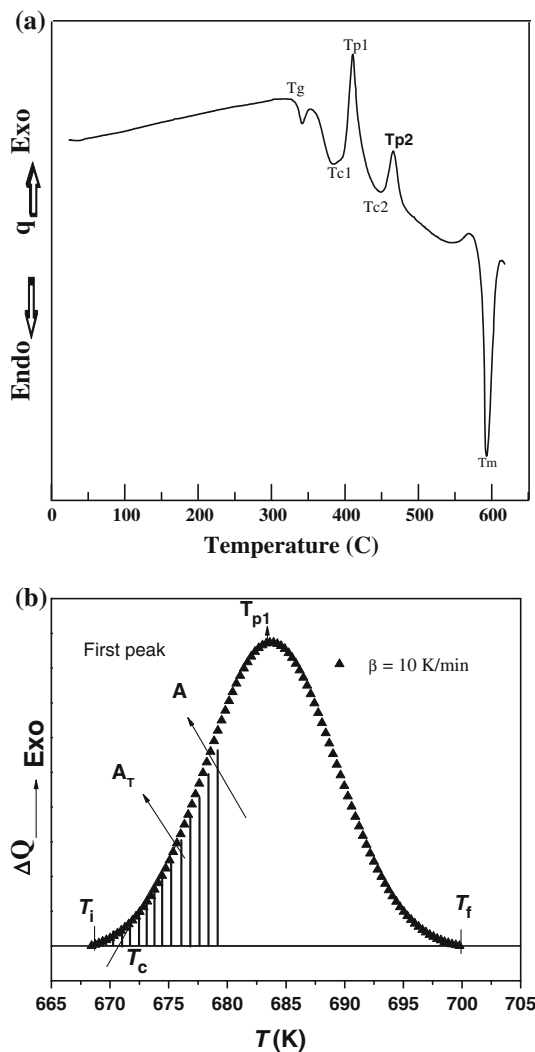


Fig. 1 The glass transition temperature with ZnO content in mol% in the prepared glasses

with equatorial position. This explains why, the glass transition temperature increase with both increasing ZnO and Bi_2O_3 content in the network glass $\text{TeO}_2/\text{Bi}_2\text{O}_3/\text{ZnO}$. Figure 2a illustrates the respective DTA thermograms of as-cast $70\text{TeO}_2 - 10\text{Bi}_2\text{O}_3 - 20\text{ZnO}$ glass sample scanned at heating rate of 10 °C/min. The glass transition (T_g), the two peaks crystallization temperature (T_{p1} and T_{p2}), and melting temperature (T_m) are marked on the thermograms. As seen in Fig. 1, DTA scan exhibits a small exothermic peak corresponding to the glass transition (T_g), and two exothermic peaks corresponds to the formation and/or transformation of crystalline phase. Onset crystallization temperature (T_c) and peak temperature of crystallization (T_p) is given in Table 1. Figure 1b depicts the DTA traces for the first crystallized peak of $70\text{TeO}_2/10\text{Bi}_2\text{O}_3/20\text{ZnO}$ at $\beta = 10$ K/min, besides the fraction, χ (crystallized at a given temperature T) given by $\chi = A_T/A$, where A is the total area of the exothermic peak between the temperatures, T_i (the onset of crystallization) and T_f (the full crystallization). A_T is the area between T_i and T . The graphical representation of the crystallized volume fraction shows the typical sigmoid curve as a function of temperature for different heating rates for the first crystallization curve $70\text{TeO}_2/10\text{Bi}_2\text{O}_3/20\text{ZnO}$ (Fig. 2a, b) based on mentioned work elsewhere [18, 19]. Figure 3 shows the plots $\ln\left(\frac{T^2}{\beta}\right)$ versus $\left(\frac{1}{T_g}\right)$ for the glass powder displaying the linearity of the equations used. The values of the activation energy obtained for the glass transition are 460.7 kJ mol⁻¹. The crystallization maximum temperature is observed to increase with the increase in heating rate (see Table 1). The crystallization maximum in DTA scans corresponds to the

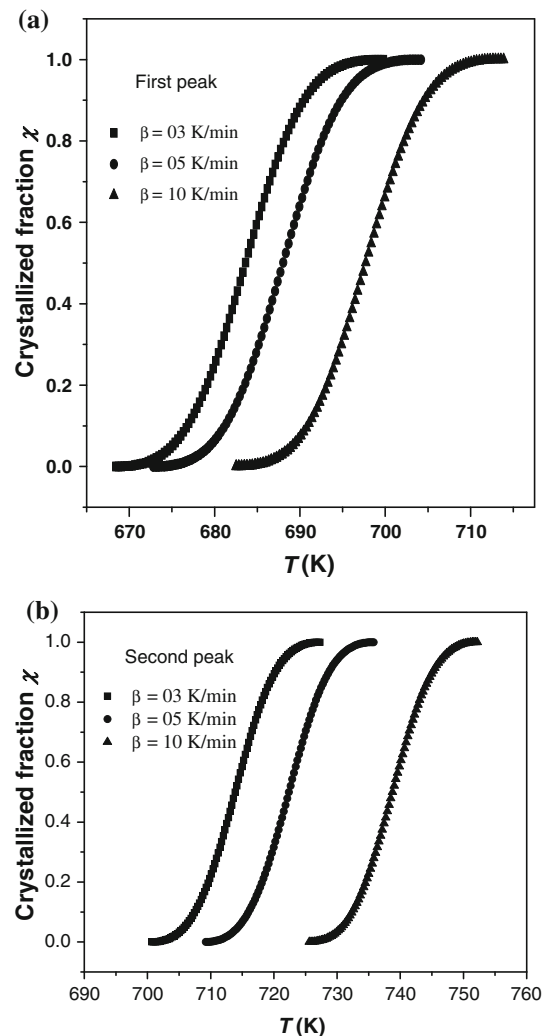
Table 1 The values of glass transition, T_g , peak of crystallization, T_p , maximum crystallization rate, and kinetic exponent for the different heating rates

β (K min $^{-1}$)	T_g (K)	T_p (K)		(d χ /dt) in 10 $^{-3}$ S $^{-1}$		First peak		Second peak	
		First peak	Second peak	First peak	Second peak	n	$\langle n \rangle$	n	$\langle n \rangle$
3	604	670	714	1.3726	1.1765	0.905	0.903	1.204	1.201
5	607	674	723	2.2518	1.9301	0.903		1.201	
10	612	684	739	4.368	3.744	0.901		1.199	

**Fig. 2** Typical DTA traces of glass 70TeO₂–10Bi₂O₃–20ZnO at 10 K min $^{-1}$

temperature at which the rate of transformation of the viscous liquid into crystals becomes maximum. This means that, the number of nucleation site is increased by using slower heating rates and the peak maximum will occur at a temperature which the melt viscosity is higher at lower temperature.

The ratio between the ordinates of the DTA curve and the total area of the peak gives the corresponding

**Fig. 3** **a** Crystallized fraction as a function of temperature at different heating rates for first crystallization curve and **b** crystallized fraction as a function of temperature different heating rates for second crystallization curve

crystallization rates, which makes it possible to build the curves of the exothermal peaks depicted in Fig. 4a, b. It was observed that, the values of $(dx/dt)_p$ increase with the increase in the heating rate. From the experimental values of the $(dx/dt)_p$, one can calculate the kinetic exponent n from Eq. 9. The value of kinetic exponent, n , for both the

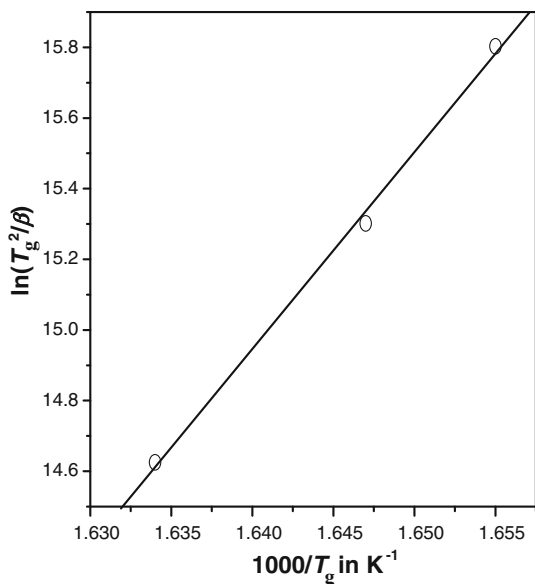


Fig. 4 Plots of $\ln\left(\frac{T_g^2}{\beta}\right)$ versus $\frac{1000}{T_p}$ of studied glass (β in $K \text{ min}^{-1}$)

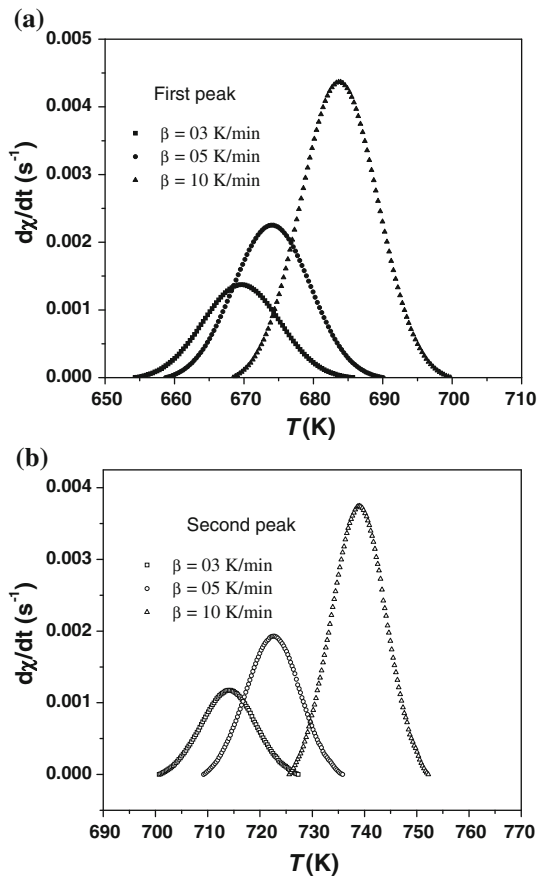


Fig. 5 **a** Crystallization rate versus temperature of the first exothermic peak at different heating rates and **b** crystallization of the second exothermic peak at different heating rates

phases at each of the experimental heating rates is given in Table 1. The value of n depends on the mechanism of the transformation reaction.

Table 2 The values of activation energy for glass transition and crystallization of $70\text{TeO}_2\text{-}20\text{ZnO}\text{-}10\text{Bi}_2\text{O}_3$

Parameter	First peak	Second peak
Activation energy of glass transition (kJ mol^{-1})	460.7	
Activation energy of crystallization (kJ mol^{-1})	305.8	197

Plot $\ln\left(\frac{T_p^2}{\beta}\right)$ versus $\left(\frac{1}{T_p}\right)$ for crystallization of the glass is shown in Fig. 5. A linear plot indicates the validity of Kissinger method [17]. The activation energy for crystallization of first phase is $305.8 \text{ kJ mol}^{-1}$, and second phase is 197 kJ mol^{-1} (see Table 2).

In order to fabricate $70\text{TeO}_2\text{-}10\text{Bi}_2\text{O}_3\text{-}20\text{ZnO}$ glass-ceramic, we applied heat treatment condition which led to the precipitation of crystalline phases. On the basis of DTA results, X-ray diffractometry scans were carried out to verify the nature of crystallizing phases in the glass network at temperature above T_g for prepared glasses. The XRD patterns for this sample at different heating temperature are shown in Figs. 6, 7. First, the $70\text{TeO}_2\text{-}10\text{Bi}_2\text{O}_3\text{-}20\text{ZnO}$ glass tempered at 350°C for 3 h [see Fig. 6 (chart a)] and 350°C for 4 h [see Fig. 6 (chart b)], it has one crystalline phase $\text{Bi}_{3.2}\text{Te}_{0.8}\text{O}_{6.4}$ (ICDD card: 00-049-1761). The important $\text{Bi}_{3.2}\text{Te}_{0.8}\text{O}_{6.4}$ was of the best solid-state oxygen ion conductors. Also, the X-ray diffractogram estimates that the same crystalline phase appears in our prepared glass tempered at 375°C for 1.5 h [see Fig. 7 (chart a)]. When the prepared glass tempered at 375°C for 3 h, two phases $\text{Bi}_{3.2}\text{Te}_{0.8}\text{O}_{6.4}$ and $\text{Zn}_2\text{Te}_3\text{O}_8$ were obtained as shown in Fig. 7 (chart b), and three crystalline phases $\text{Bi}_{3.2}\text{Te}_{0.8}\text{O}_{6.4}$, $\text{Zn}_2\text{Te}_3\text{O}_8$ (ICDD card: 20-1270), $\text{Bi}_2\text{Te}_4\text{O}_{11}$ (ICDD card: 01-081-1330), respectively, were obtained, when it tempered 375°C for 4.5 h as shown in

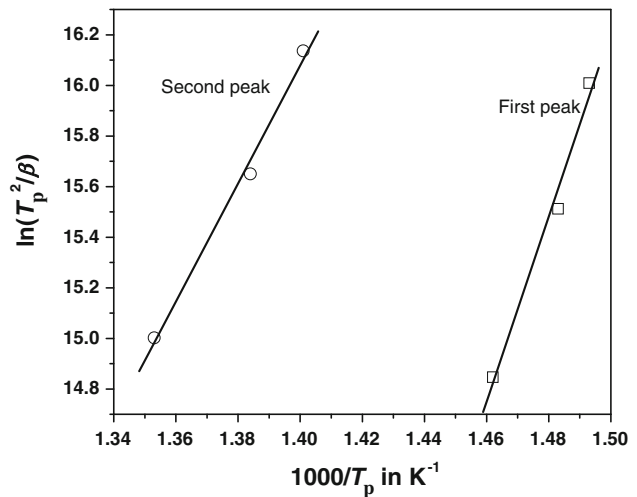


Fig. 6 Plots of $\ln\left(\frac{T_p^2}{\beta}\right)$ versus $\frac{1000}{T_p}$ of studied glass (β in $K \text{ min}^{-1}$)

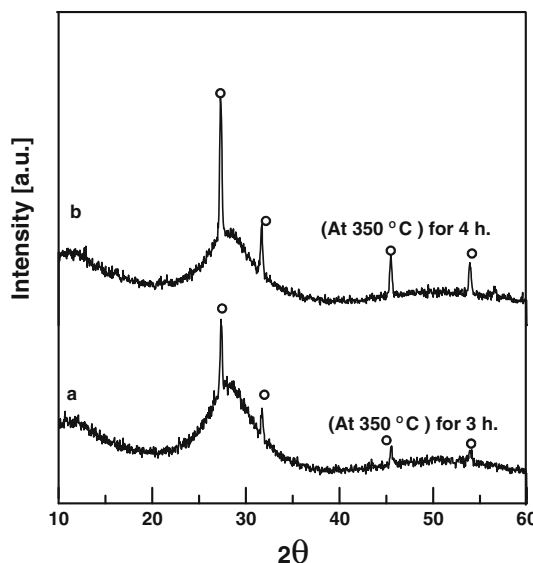


Fig. 7 XRD patterns of tempered sample 70TeO₂–10Bi₂O₃–20ZnO (chart *a*, 350 °C/3 h), (chart *b*, 350 °C/4 h) (open circle) Bi_{3.2}Te_{0.8}O_{6.4}

Fig. 8 (chart c). Furthermore, heat treatment at higher temperature leads to the complete reaction of Bi₂O₃ with TeO₂ to form the stoichiometric compound Bi₂Te₄O₁₁. Senthil Murugan et al. [12] estimated the primary phase Bi_{3.2}Te_{0.8}O_{6.4} which belongs to the cubic (centro symmetric) phase along with traces of Bi₂TeO₅ in the 70TeO₂–15Bi₂O₃–15ZnO glass heat treated at 350 °C/6 h. Also, they were found only major phase Bi₂Te₄O₁₁ in the same sample heat treated at 500 °C/6 h. Kozhukharov et al. [20] estimated the phase of α -TeO₂ at the temperature 435 °C and Te₃Zn₂O₈ at 479 °C for 80 mol% TeO₂ and 20 mol% ZnO composition and concluded the crystallizing Zn₂Te₃O₈ phase only at 432 ° in the 60 mol% TeO₂ and 40 mol% ZnO, which corresponds to single crystallization peak. It is well known that in the Zn₂Te₃O₈ structure ${}^1_{\infty}[\text{Te}(4)\text{Te}_2(3+1)\text{O}_8]$ chains are formed where for one TeO₄ polyhedron, there are two TeO₃ trigonal pyramids. Popple et al. [21] detected Bi₂Te₄O₁₁ phase in the Bi₂O₃–TeO₂. Moreover, the TeO₂ evaporates onto the Bi₂O₃ grains producing TeO₂ layer, and hence this TeO₂ layer reacts with the Bi₂O₃ by bulk diffusion forming Bi₂Te₄O₁₁ reactions. From the previous reported data, we conclude that, Bi_{3.2}Te_{0.8}O_{6.4}, Zn₂Te₃O₈, and Bi₂Te₄O₁₁ reactions also are taking place by bulk diffusion in our glasses, not new crystalline phases appeared in prepared glass. Furthermore the activation energy of obtained crystalline phases in the prepared glass are 305.8 and 197 kJ mol^{−1} and the kinetic parameter, *n*, for both crystallization exotherms closed to 1.0 (i.e., one dimensional growth from surface to inside).

The prepared glasses are high homogeneity transparent glass-ceramics depending on the heat treatment condition.

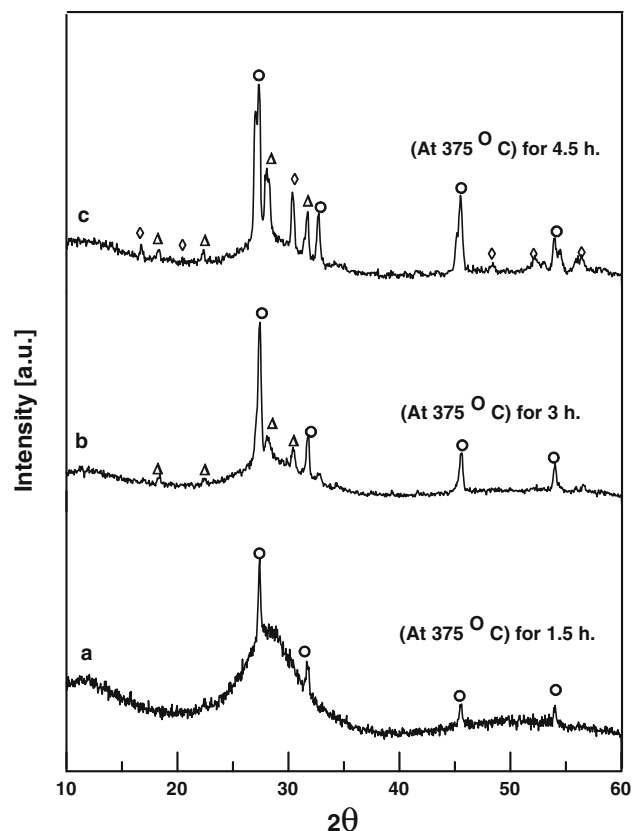


Fig. 8 XRD patterns of tempered sample 70TeO₂–10Bi₂O₃–20ZnO (chart *a*, 375 °C/1.5 h), (chart *b*, 375 °C/3 h), (chart *c*, 375 °C/4.5 h), (open circle) Bi_{3.2}Te_{0.8}O_{6.4}, (open triangle) Zn₂Te₃O₈ and (open rhombus) Bi₂Te₄O₁₁

Therefore, it is easy to take the photos of crossed polarized transmission microscope for the 70TeO₂–10Bi₂O₃–20ZnO glass at different heating temperature are shown in Fig. 9a–e. It has high-nucleation density of crystallites when tempered at 350 °C at different times 1, 2, 3, and 4 h. (see Fig. 9a–e). Also, the grain size of crystallites increases with increasing the time of sample thermally treated. The prepared sample was examined under transmission electron microscope (TEM) after sputtering a thin carbon film on the prepared glass for conduction. The TEM micrographs for this sample were shown in Fig. 10a–d, which indicate that the scattered crystallites are uniform size in range 5 μm in the prepared sample tempered at 350 °C/4 h. Also, Fig. 10a revealed centrosymmetric tridymite crystal in the matrix of the prepared glass. Figure 10b is TEM micrograph of the sample 70TeO₂–10Bi₂O₃–20ZnO heated 400 °C for 0.5 h, which reveals crystalline phase, droplet-free halos and amorphous glassy regions in the microstructure. When Bi₂O₃ is added in tellurite glasses, it contributes the following effects: (i) incorporation of holes and defects between two chains, (ii) formation of strong Te–O–M ion covalent bonds, and (iii) strong influence on the Te–axOeq–Te angle between two polyhedra and distorted in TeO_{3±1} unit followed by a

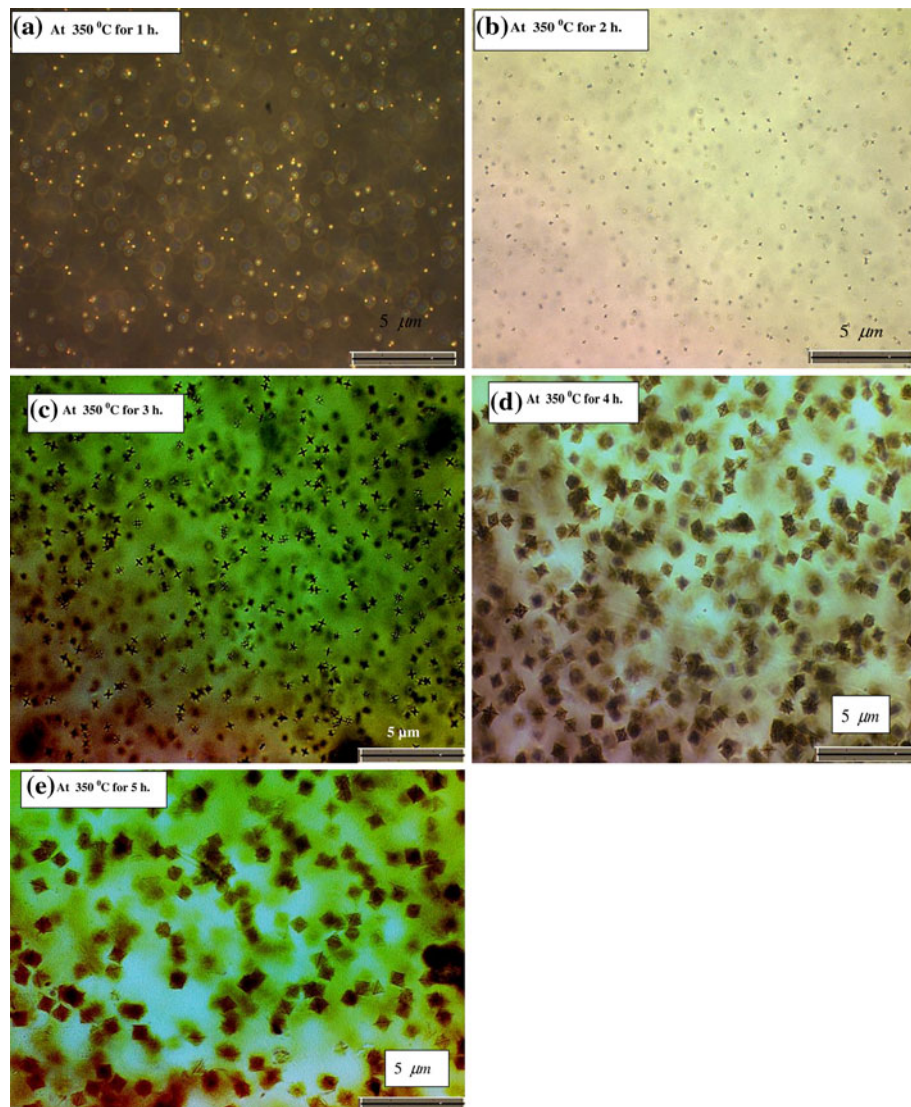


Fig. 9 Polarized optical micrographs of sample 70TeO₂–10Bi₂O₃–20ZnO: **a** 350 °C/1 h, **b** 350 °C/2 h, **c** 350 °C/3 h, **d** 350 °C/4 h, **e** 350 °C/5 h

creation of regular TeO₃ trigonal pyramid units leaving non-bridging oxygen atoms and due to the formation of Te–O–Bi kingies in the glass matrix [22–25]. So, we are suggest that when addition of Bi₂O₃ to the TeO₂–ZnO glasses causes splitting of O–Te–O and Zn–O–Zn bonds and hence, the bridging oxygens (BO) are converted into non-bridging oxygens (NBO) and the electronic shell of O²⁻ ion is affected by polarizing action of modifying ions, since Bi³⁺ ions are highly polarizing with Te⁴⁺. This is due to droplet holes formed in the glass-ceramic matrix of present sample.

At temperature 375 °C for 3 h, the matrix of glass has high dense needle shaped crystal is shown in Fig. 10c. Finally, we found that, Bi³⁺ played an important role to get crystallization in the tellurite glass-ceramic by using mapping TEM of glassy ceramic matrix of 70TeO₂–10Bi₂O₃–20ZnO.

Conclusion

From the present study of TeO₂/ Bi₂O₃/ZnO glasses, it is observed that the glass transition increase with increasing ZnO and Bi₂O₃ content. A highly transparent glass-ceramics can be successfully obtained by controlling the heat treatment precisely. The phase separation and crystallization kinetics in 70TeO₂–10Bi₂O₃–20ZnO were investigated. It was found that the phase separation in the present glass occurs at 400 °C/0.5 h. The activation energies of crystallization were calculated to be 305.8 and 197 kJ mol⁻¹ for first and second crystallization exotherms, respectively. Moreover, synthesized crystalline phases Bi_{3.2}Te_{0.8}O_{6.4}, Bi₂Te₄O₁₁, Zn₂Te₃O₈, respectively, were investigated.

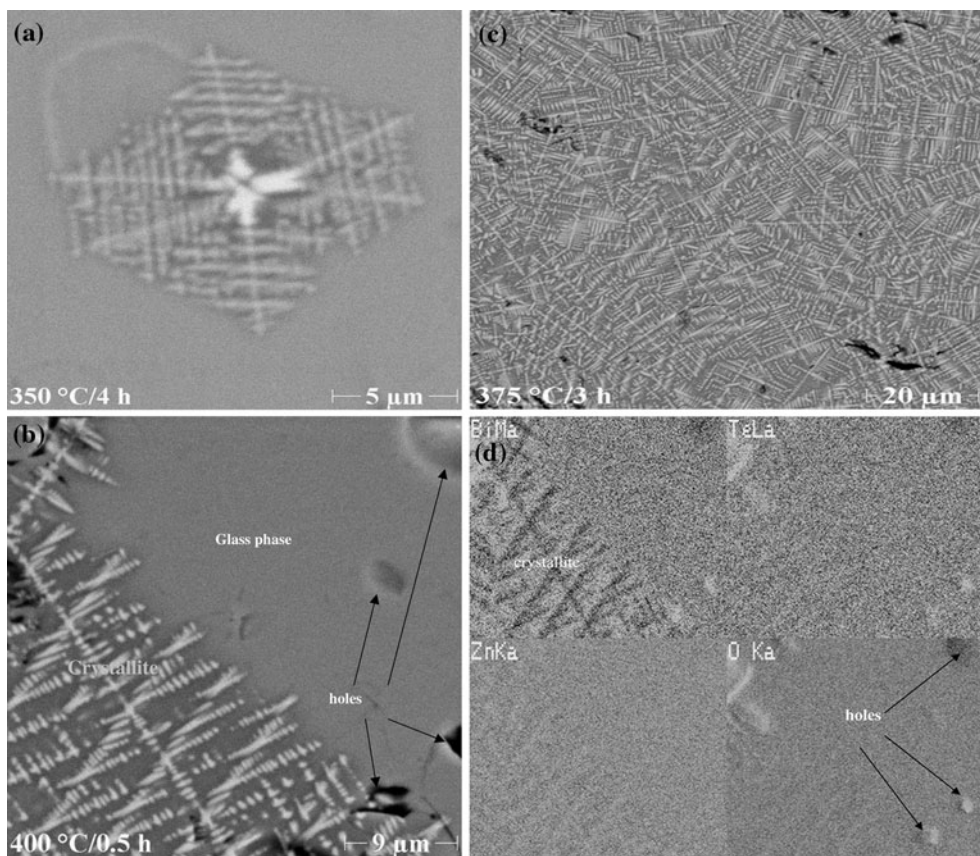


Fig. 10 TEM microphotograph of sample $70\text{TeO}_2\text{-}10\text{Bi}_2\text{O}_3\text{-}20\text{ZnO}$: **a** $350\text{ }^\circ\text{C}/4\text{ h}$, **b** $400\text{ }^\circ\text{C}/0.5\text{ h}$, **c** $375\text{ }^\circ\text{C}/3\text{ h}$, and **d** Mapping analysis of glass-ceramics for this sample

Acknowledgements E. Yousef wishes to thank Professor C. Russel Otto Schott Institute, Friedrich Schiller University Jena Germany for interest in this work and helpful.

Open Access This article is distributed under the terms of the Creative Commons Attribution Noncommercial License which permits any noncommercial use, distribution, and reproduction in any medium, provided the original author(s) and source are credited.

References

- El-Mallawany R (2002) Tellurite glasses handbook: physical properties and data. CRC Press, Boca Raton
- Lenher V, Wolessensky E (1913) J Am Chem Soc 35:718
- Stanworth J (1952) J Soc Glass Technol 36:217
- Sigaev VN, Sarkisov PD, Kupriyanova MV, Spiridonov YA, Lopatina EV, Stefanovich SY, Molev VI, Pernice P, Aronne A (2001) Glass Phys Chem 27:497
- Hoppe U, Yousef E, Russel C, Neufeind J, Hannon AC (2004) J Phys Condens Matter 16:1654
- Sigaev VN, Pernice P, Aronne A, Akimova OV, Stefanovich SY, Scaglione A (2001) J Non-Cryst Solids 292:59
- Kim HG, Komatsu T, Sato R, Matusita K (1993) J Non-Cryst Solids 162:201
- Kazuhide S, Komatsu T, Kim HG, Sato R, Matusita K (1995) J Non-Cryst Solids 189:16
- Komatsu T, Shioya K (1997) J Non-Cryst Solids 209:305
- Tromel M, Munch E (1985) J Less-Common Met 110:421
- Sato R, Benino Y, Fujiwara T, Komatsu T (2001) J Non-Cryst Solids 289:228
- Senthil Murugan G, Fargin E, Rodriguez V, Adamietz F, Couzi M, Buffeteau T, Le Coustumer P (2004) J Non-Cryst Solids 344:158
- Johnson WA, Mehl RF (1939) Trans AIME 135:419
- Avrami M (1939) J Chem Phys 7:1103
- Khan SA, Zulfequar M, Husain M (2002) J Phys Chem Solids 123:463
- Goel MA, Shaaban ER, Melo FCL, Ribeiro MJ, Ferreira JM (2007) J Non-Cryst Solids 353:2383
- Kissinger HE (1957) Anal Chem 29:1702
- Shaaban ER, Ishu Kansal M, Shapaan JM, Ferreira F (2009) J Thermal Anal Calorim 98:354
- Shaaban ER, Dessouky MT, Abousehly AM (2008) J Philos Mag 88(7):1099
- Kozhukharov V, Burger H, Neov S (1986) J Polyhedron 5(3): 771
- Popple L, Zsuzsanna S (2003) J Thermal Anal Calorim 74:375
- Neov S, Kozhukharov V, Gerasimov I, Krezhov K, Sidzhimov B (1979) J Phys Solid State 12:2475
- Rajendran V, Palanicely N, Chaudhuri BK, Goswami K (2003) J Non-Cryst Solids 320:195
- Reddy RR, Nazeer Ahmed Y, Abdul Azeem P, Rama K (2001) J Non-Cryst Solids 286:169
- Hanke K (1967) Naturwissenschaften 54:199